

LA-UR-12-24946

Approved for public release; distribution is unlimited.

Title: A detailed study of the nuclear dependence of the EMC Effect and Short-Range Correlations

Author(s): Fomin, N
Arrington, J.
Daniel, A.
Day, D.B.
Gaskell, D
Solvignon, P.

Intended for: Physical Review C



Disclaimer:

Los Alamos National Laboratory, an affirmative action/equal opportunity employer, is operated by the Los Alamos National Security, LLC for the National Nuclear Security Administration of the U.S. Department of Energy under contract DE-AC52-06NA25396. By approving this article, the publisher recognizes that the U.S. Government retains nonexclusive, royalty-free license to publish or reproduce the published form of this contribution, or to allow others to do so, for U.S. Government purposes. Los Alamos National Laboratory requests that the publisher identify this article as work performed under the auspices of the U.S. Department of Energy. Los Alamos National Laboratory strongly supports academic freedom and a researcher's right to publish; as an institution, however, the Laboratory does not endorse the viewpoint of a publication or guarantee its technical correctness.

A detailed study of the nuclear dependence of the EMC Effect and Short-Range Correlations

J. Arrington,¹ A. Daniel,^{2,3} D. B. Day,³ N. Fomin,⁴ D. Gaskell,⁵ and P. Solvignon⁵

¹*Physics Division, Argonne National Laboratory, Argonne, IL, 60439, USA*

²*Ohio University, Athens, OH, 22801, USA*

³*University of Virginia, Charlottesville, VA, 22904, USA*

⁴*Los Alamos National Laboratory, Los Alamos, VA, 87545, USA*

⁵*Thomas Jefferson National Laboratory, Newport News, VA, 23606, USA*

(Dated: June 14, 2012)

Background: The density of the nucleus has been important in explaining the nuclear dependence of the quark distributions, also known as the EMC effect, as well as the presence of high-momentum nucleons arising from short-range correlations (SRCs). Recent measurements of both of these effects on light nuclei have shown a clear deviation from simple density-dependent models.

Purpose: A better understanding of the nuclear quark distributions and short-range correlations requires a careful examination of the experimental data on these effects to constrain models that attempt to describe these phenomena.

Methods: We present a detailed analysis of the nuclear dependence of the EMC effect and the contribution of SRCs in nuclei, comparing to predictions and simple scaling models based on different pictures of the underlying physics. We also make a direct, quantitative comparison of the two effects to further examine the connection between these two observables related to nuclear structure.

Results: We find that, with the inclusion of the new data on light nuclei, neither of these observables can be well explained by common assumptions for the nuclear dependence. The anomalous behavior of both effects in light nuclei is consistent with the idea the the EMC effect is driven by either the presence of high-density configurations in nuclei or the large virtuality of the high-momentum nucleons associated with these configurations.

Conclusions: The unexpected nuclear dependence in the measurements of the EMC effect and SRC contributions appear to suggest that the local environment of the struck nucleon is the most relevant quantity for explaining these results. The common behavior suggests a connection between the two seemingly disparate phenomena, but the data do not yet allow for a clear preference between models which aim to explain this connection.

PACS numbers: 25.30Fj, 13.60Hb

INTRODUCTION

The nucleus is a system of strongly-interacting protons and neutrons. The characteristic scale for the nucleon momentum is the Fermi momentum, $k_F \approx 200\text{--}270$ MeV/c, a consequence of the interaction of the nucleon with the mean field of the nucleus. The strongly repulsive feature of the nucleon-nucleon (NN) interaction at short distances prevents two nucleons from becoming very close to each other and this loss of configuration space demands the existence of high-momentum components in the nuclear ground state wavefunction. These can not be described in the context of mean field models and are commonly called short-range correlations (SRCs). Inelastic electron scattering was suggested long ago [1] to be a source of qualitative information on SRCs, yet they remain one of the least-well characterized aspects of the structure of stable nuclei.

Knockout reactions studied in inclusive and exclusive electron scattering [2–9] have isolated SRCs by probing the high-momentum tail of the nuclear momentum distribution in nucleon knock-out reactions. The high momentum tail is assumed to be the result of short-range

hard interactions between nucleons [2, 10, 11], allowing a study short-distance structure via reactions with high-momentum nucleons. The strength of SRCs in the nucleus has long been assumed to scale with nuclear density, a proxy for the probability of two nucleons interacting at short distances.

Typical parameterizations of the repulsive core of the NN interaction [12–14] show a sharp rise in the potential well below 1 fm. Because the nucleon has an RMS radius of roughly 0.85 fm [15], nucleons can have significant overlap. In heavy nuclei, the typical inter-nucleon separation is 1.6 fm, suggesting that the nucleons have some overlap most of the time, and this short-range interaction may cause a modification of the structure of the nucleon. There is a long history of searches for this kind of “medium modification” of nucleon structure through measurements of the in-medium nucleon form factors [16–18] or modification of the quasielastic response in nuclei [19–23]. Overlap of the nucleons may also allow for direct quark exchange, providing a new mechanism for modifying quark momentum distributions in the nucleus. Thus, one may expect quark momentum distributions in nuclei, like SRCs, to have a dependence

on the average nuclear density.

This was first observed by the EMC collaboration [24] and is commonly referred to as the EMC effect. It was discovered that the per nucleon cross section in the DIS regime was different for iron and the deuteron. Because the binding energy of nuclei is extremely small compared to the energy scales in the deep-inelastic scattering used to probe the quark distributions, the early assumption was that the parton distribution functions (pdfs) of the nucleus would be a simple sum of the proton and neutron pdfs, except at the largest values of the quark momentum fraction (Bjorken- x) where the Fermi motion of the nucleus becomes important. Since the DIS cross sections depend on the quark distributions, the difference in the measured cross sections for iron and the deuteron indicated a suppression of quark pfs in nuclei for $0.3 < x < 0.7$, and the size of this effect was seen to scale with the nuclear density.

Thus, the density of the nucleus has often been taken as the driving parameter of both the A dependence of the nuclear pdfs and the presence of short-distance configurations in nuclei which give rise to high-momentum nucleons. This relationship was recently quantified [25], via a linear correlation between the SRCs in the tail of the nucleon momentum distribution and the size of the EMC effect. This is consistent with the idea that both effects scale with nuclear density, and provides a direct connection that does not rely on the evaluation of the nuclear densities.

In addition to the density-driven picture, other explanations of the EMC effect have been proposed as well [26, 27]. While the measurements performed in the '80s and '90s were well described by a density-dependent fit [28], the weak A dependence for these nuclei could be equally well described in other approaches. For example, some works have explained the effect in terms of average virtuality ($\nu = p^2 - m_N^2$) of the nucleons [10, 29, 30], connecting it more closely to the momentum distributions. Given the limited precision of the EMC effect measurements and the fact that its proposed governing quantities all grow smoothly but slowly for heavy nuclei, it is difficult to make a clear determination of which approaches best described the A dependence of the EMC effect.

Recent measurements focusing on light nuclei [7, 31] have observed a clear breakdown of the density-dependent picture for both the EMC effect and the strength of short-range correlations in nuclei. In this work, we provide a detailed analysis of the nuclear dependence of these two quantities, focusing on comparisons to model-inspired assumptions. We present an extended version of the analysis presented in Refs. [25, 32], including these new data which violate the simple density-dependent scaling observed for heavier nuclei. For both the analysis of the A dependence and the direct comparison of the EMC and SRC data, we examine in more detail the meaning of the observables associated with these

effects. As the underlying dynamics behind the examination of the direct correlation differ, additional corrections may be required when comparing the observables that are typically associated with the EMC effect or presence of SRCs.

NUCLEAR DEPENDENCE OF THE EMC EFFECT

Deep Inelastic Scattering (DIS) provides access to the quark distributions in nuclei via measurements of inclusive cross sections. This cross section for electron or muon scattering from a nucleus can be written as

$$\frac{d\sigma}{dx dQ^2} = \frac{4\pi\alpha^2 E'^2}{xQ^4} \frac{E'}{E} \left[F_2 \cos^2 \frac{\theta}{2} + \frac{2\nu}{M} F_1 \sin^2 \frac{\theta}{2} \right], \quad (1)$$

where F_1 and F_2 depend on x and Q^2 . In the quark-parton model, information about the quark distribution functions is encoded in the inelastic F_1 and F_2 structure functions. In the Bjorken limit (Q^2 and $\nu \rightarrow \infty$, fixed $\frac{\nu}{Q^2}$), we have,

$$F_1(x) = \frac{1}{2} \sum_q e_q^2 q(x), \quad F_2(x) = 2xF_1, \quad (2)$$

where $q(x)$ is the quark distribution function and e_q is the quark charge for a given flavor (u, d, s).

The per-nucleon ratio of the F_2 structure functions between an isoscalar nucleus and the deuteron is then a direct measure of the modification of quark distributions in nuclei. Experimentally, this ratio is defined $R_{EMC} = (F_2^A/A)/(F_2^D/2)$. The deuteron structure function in the denominator is taken to approximate the sum of free proton and neutron structure functions. In almost all measurements of the EMC effect, an additional assumption is made that the ratio of longitudinal to transverse cross sections, $R = \sigma_L/\sigma_T$, is A -independent such that the unseparated ratio of cross sections corresponds directly to the F_2 ratio, i.e., $\sigma_A/\sigma_D = F_2^A/F_2^D$. For non-isoscalar nuclei an additional correction is typically applied to account for the difference in DIS cross sections between protons and neutrons.

Figure 1 shows a measurement of the EMC ratio for carbon from Ref. [31]. The region from $x = 0.3$ to 0.7 shows the depletion in the cross section ratio characteristic of all nuclei. The increase of the cross section ratio at large x is attributed to the greater Fermi momentum in the heavy nucleus as compared to the deuteron. The shape of the EMC ratio appears to be universal, independent of nucleus, while the magnitude of the high- x suppression generally increases with A .

The origin of the EMC effect has been a topic of intense theoretical discussion since its original observation. There have been many explanations proposed, and these can be broadly broken down into two categories. Some

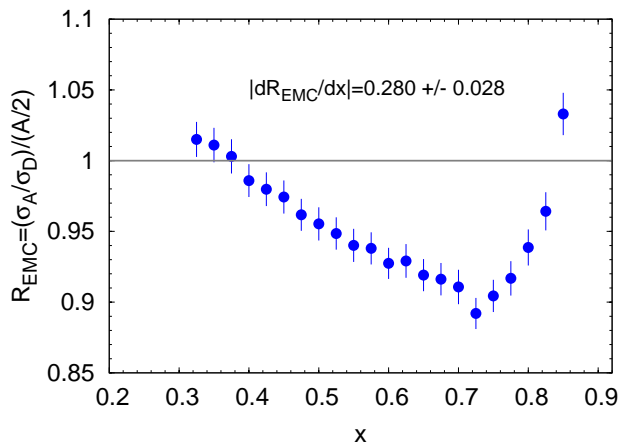


FIG. 1: (color online) EMC ratio, $(\sigma_A/A)/(\sigma_D/2)$, for carbon [31].

approaches include only “traditional” nuclear physics effects, using convolution models which include binding effects, detailed models of the nucleon momentum distribution, or pion-exchange contributions. Other calculations invoke more exotic explanations such as re-scaling of quark distributions in the nuclear environment, contributions of six or nine quark bags, or modification of the internal structure of the nucleons such as “nucleon swelling” or suppression of point-like nucleon configurations. Several review articles give an overview of models of the EMC effect, see for example [26, 27, 33].

Despite this abundance of models, there is no firm consensus as to the origin of the EMC effect. The observed suppression of the F_2 structure function between $0.3 < x < 0.7$ is relatively straightforward to reproduce in a variety of approaches. A study of the effect as a function of A should allow for more stringent tests of these models and provide important clues as to its fundamental origin.

In the following, we discuss some previous approaches to examining the nuclear dependence of the EMC effect. We use the data from SLAC E139 [28] and the recent data on light nuclei from Jefferson Lab E03-103 [31]. SLAC E139 sampled a range of nuclei from $A = 4$ to 197, allowing a large lever arm for studying the nuclear dependence. Jefferson Lab experiment E03-103 adds ^3He and additional precise data on ^4He , ^9Be , and ^{12}C .

We use the definition of the “size” of the EMC effect as introduced in [31], i.e., we define the magnitude of the EMC effect to be $|dR_{EMC}/dx|$, the value of the slope of a linear fit to the cross-section ratio for $0.35 < x < 0.7$. These limits were chosen to give a range of high precision data whose behavior was linear. The slope was also extracted over other ranges in x and the nuclear dependence of the slopes did not vary significantly. This definition reduces the sensitivity to normalization errors, which would otherwise be significant if one were to assess the nuclear dependence at a fixed value of x , especially for

light nuclei. The impact of normalization uncertainties for the deuteron measurements (common to all ratios in a given experiment) are also reduced in this approach. This procedure makes use of the fact that the EMC effect has a universal shape for $x > 0.3$, exhibited by all experimental data.

Table I lists the EMC slopes extracted from the two data sets used in the analysis presented in this paper. We do not include data from earlier measurements due to their relatively poor precision and/or limited x -coverage.

TABLE I: Combined EMC results from JLab E03-103 [31] and SLAC E139 [28] (averaged over Q^2). For JLab data, $|dR_{EMC}/dx|$ was extracted in the $0.35 \leq x \leq 0.7$ range. SLAC data, whose binning was different, were fit over $0.36 \leq x \leq 0.68$. For both cases, statistical and point-to-point systematic uncertainties were applied to each x -bin and the normalization uncertainties (including the 1% normalization uncertainty on deuteron common to all ratios for the SLAC data) were applied to the extracted slope.

A	JLab	SLAC	Combined
^3He	0.070 ± 0.028	–	0.070 ± 0.028
^4He	0.198 ± 0.027	0.191 ± 0.061	0.197 ± 0.025
Be	0.271 ± 0.030	0.208 ± 0.038	0.247 ± 0.023
C	0.280 ± 0.029	0.318 ± 0.041	0.292 ± 0.023
Al	–	0.325 ± 0.034	0.325 ± 0.034
^{40}Ca	–	0.350 ± 0.047	0.350 ± 0.047
Fe	–	0.388 ± 0.032	0.388 ± 0.033
Ag	–	0.496 ± 0.051	0.496 ± 0.052
Au	–	0.409 ± 0.039	0.409 ± 0.040

An effect not yet discussed is that of Coulomb distortion [34]. The influence of the Coulomb field of the nucleus on the incident or scattered lepton is a higher order QED effect, but is not typically included in the radiative corrections procedures. Since the size of the effect (and the associated correction) depends on Z , it is potentially important when considering the nuclear dependence of the EMC effect. In addition, the EMC effect is taken directly from the cross section ratio instead of the structure function ratio, thus assuming no nuclear dependence in $R = \frac{\sigma_L}{\sigma_T}$. Coulomb distortions introduce kinematical corrections and consequently have a direct effect on the extraction of R . An indication of nuclear dependence in R was observed recently [35] after applying Coulomb corrections to SLAC E139 and E140 [36] data.

The JLab data have been corrected for both Coulomb distortion and non-isoscalar effects. For the SLAC data, Coulomb distortion was not included, but is estimated to be negligible for nuclei lighter than ^{12}C and at most a 2% effect on the ^{197}Au EMC slope. These changes do not significantly affect the nuclear dependencies studied below. The JLab and SLAC data sets were analyzed using different prescriptions to correct non-isoscalar nuclei. In the case of SLAC data, a simple, x -dependent parametrization was employed based on high Q^2 data for F_2^D/F_2^P .

A more sophisticated correction was applied to the JLab data, using a smeared ratio of free proton and neutron cross sections [31]. Reanalysis of the SLAC data using the updated isoscalar corrections yields slightly higher EMC slopes for the very heavy nuclei, but does not impact the overall conclusions of this analysis. A detailed comparison of these effects for both the SLAC data and the heavy target data from JLab E03-103 are in progress [37, 38].

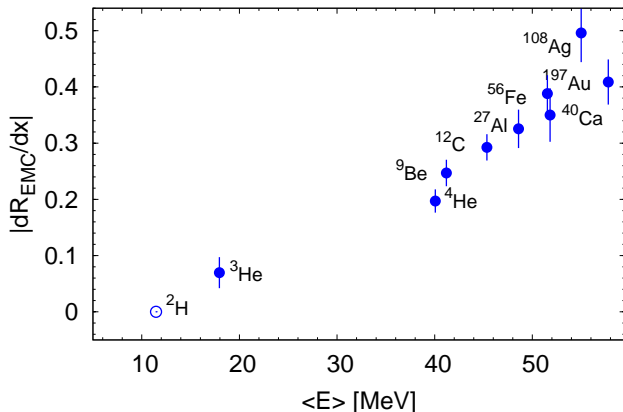


FIG. 2: (color online) Magnitude of the EMC effect, defined as $|dR_{EMC}/dx|$ vs. the mean nucleon separation energy, $\langle \epsilon \rangle$. The empty circle shows zero expected EMC effect for the deuteron (not a measured quantity). The separation energies are calculated using spectral functions from [39, 40].

Initial efforts to describe the EMC effect within a convolution model were unsuccessful. However, any attempt to explain the EMC effect must include the role of the convolution, which, while small, has a similar trend, growing with A . Ideally, one could remove the convolution contribution to the A dependence which we should to study. We have not done this as it would have a minimal impact on the A dependence, while introducing an unwanted model dependence.

Since the convolution picture approach is unable to give a significant suppression at large x , it was proposed that the inclusion of binding effects was required to provide a more complete description. Ref. [41] gives an excellent overview of early calculations of the EMC effect in the binding approach. One can examine the dependence of EMC effect on the binding energy per nucleon, E_A/A . However, this does not describe the data well as the binding energy peaks near $A = 56$ and decreases for both heavier and lighter nuclei. Additionally, one can look at minimum separation energy, which is what is required to remove a nucleon from the outer shell. However, electron scattering samples all the nucleons, leading us to look at a different energy quantity.

The heart of the binding model describes nucleons bound in a nucleus with some non-zero three-momentum, and as a consequence of the nuclear binding, an energy modified from its usual on-shell value,

i.e., $E_N \neq \sqrt{p_N^2 + m_N^2}$. The bound nucleon has a removal or separation energy ϵ , with its total energy given by $E_N = m_N + \epsilon$ (ignoring the kinetic energy of the recoiling nucleus). In practice the average separation energy is often determined using the Koltun sum rule [42],

$$\langle \epsilon \rangle + \frac{\langle p^2 \rangle}{2m_N} = 2 \frac{E_A}{A}, \quad (3)$$

where p is the nucleon three-momentum and E_A/A is the binding energy per nucleon. The modification to the nucleon energy results in a value of $x = Q^2/2p_N \cdot q$ shifted by $\approx \langle \epsilon \rangle / m_N$. This approach was rather successful in reproducing the shape of the EMC effect at large x [43, 44].

In this context, the EMC effect comes about due to the fact that the nucleon is off-shell, but the binding effect results in a simple rescaling of the relevant kinematic variable (x) and does not imply an inherent modification of the nucleon structure in the nucleus.

Figure 2 shows the extracted EMC ratio as a function of the average nucleon separation energy, $\langle \epsilon \rangle$ from [45]. In this figure, the separation energy was calculated from spectral functions used and described in [39, 40]; the spectral functions in this calculation include contributions from both mean-field and correlated (high momentum) components of the nuclear wave function. While the separation energy is an inherently model-dependent quantity, we have investigated alternate descriptions and found agreement to usually better than 5 MeV. This calculation is shown in Fig. 2, providing the most complete set of nuclei and the best description of the data. While qualitatively the size of the EMC effect correlates very well with the average separation energy, this description does not work for all nuclei. Nuclear binding models have failed to gain traction in the past, usually due to the omission of the so-called “flux factor” (incorrect treatment of wave-function normalization), exclusion of pions [29], and failure to describe the Drell-Yan data. included somehow whenever nuclear binding is discussed”

It has been argued that the average separation energy should be replaced with binding energy per-nucleon in the rescaling of x described above [46, 47]. Since the binding energy is significantly smaller than the average separation energy (~ 9 MeV vs. 51 MeV for iron) the resulting kinematic shift is much too small to fully account for the EMC effect. Nonetheless, we have examined the correlation between the size of the EMC effect and binding energy, E_A/A , and found that a linear fit yields a poor χ^2_ν value and a poor description of the data.

It is unlikely that the modification of the nucleon pdfs in the nucleus can be explained by binding effects alone, and aspects of medium modification must be included [29, 39, 48].

The E139 analysis [28] examined the nuclear dependence of the EMC effect in terms of an ad-hoc logarithmic A -dependence and the average nuclear density. In

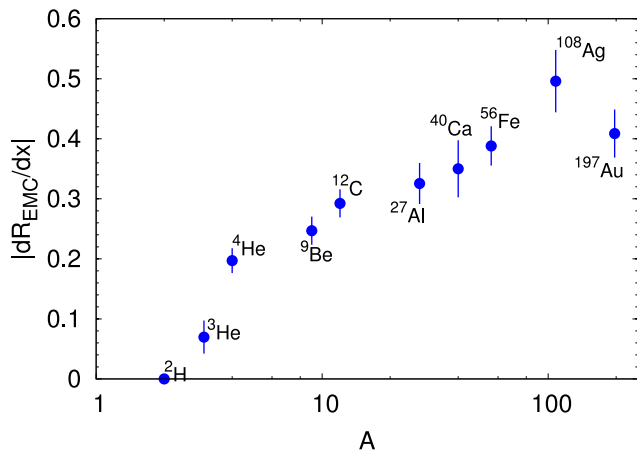


FIG. 3: (color online) Magnitude of the EMC effect vs. A .

Fig. 3 we show the EMC data vs. A . There is no particular expectation that the EMC effect should correlate logarithmically with A , although, as was seen in [28], the assumption works remarkably well for large A . However, as one moves away from large A , there is a significant deviation for $A = 3$. Alternatively, an A dependent fit could be constructed from the values of $A < 12$, but this would then fail at larger A . When including light nuclei, examining the EMC effect versus $\ln(A - 1)$ may be more appropriate as it gives the correct limit for $A = 2$. However, while this improves the quality of the fit somewhat for light nuclei, it still does not provide an acceptable description of the full data set.

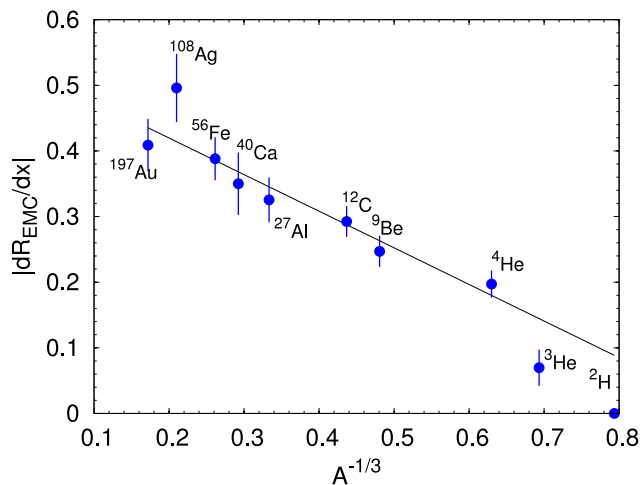


FIG. 4: (color online) Magnitude of the EMC effect vs. $A^{-1/3}$ as well as a linear fit for $A \geq 12$.

Exact nuclear matter calculations [49] can be applied to finite nuclei within the local density approximation (LDA)[50, 51]. This provides an estimate of the A dependence for effects that depend on the nuclear density and is based on general characteristics of the nuclear density distributions. For nuclei with $A > 12$ the nuclear den-

sity distribution $\rho(r)$ has a common shape and has been found to be relatively constant in the nuclear interior. Contributions to the lepton scattering cross section from this portion of the nucleus should then scale with A . The nuclear surface is also characterized by a nearly universal shape, $\rho(r - R)$, where R is the half-density radius $R = r_0 A^{1/3}$, such that contributions from the surface grow as R^2 , or $A^{2/3}$. It then follows that the cross section per nucleon should scale like $A^{-1/3}$. For small- A nuclei the nuclear response is dominated by surface effects while for large- A nuclei the nuclear response is dominated by the constant density region. It has been argued that the response function (per nucleon) for nuclear matter can be extrapolated as a linear function of $A^{-1/3}$ to $A^{-1/3} = 0$ in the deep inelastic scattering region [51].

In Figure 4 the extracted EMC slope is plotted versus $A^{-1/3}$. Somewhat surprisingly, this yields one of the better correlations with the data, even for very light nuclei. This is not expected, since the prediction of the $A^{-1/3}$ behavior is based on the assumption of an A -independent “surface” density distribution and a scaling with A of the volume/surface ratio. The assumption that the shape of the “surface” density is universal is certainly not valid for $A \leq 12$, and it is not clear that the division into a surface region and a high-density core is at all applicable to ${}^3\text{He}$ or ${}^4\text{He}$.

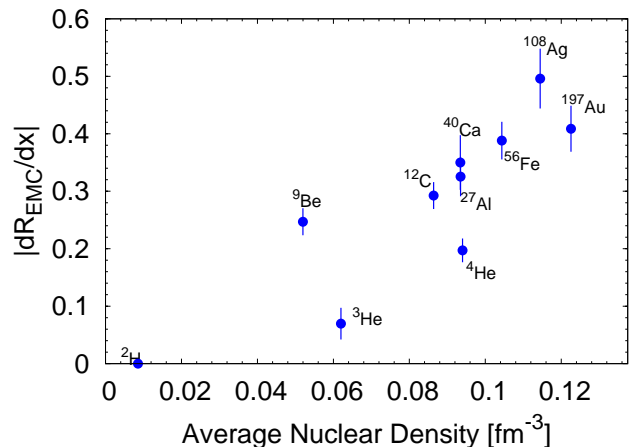


FIG. 5: (color online) Magnitude of the EMC effect vs. average nuclear density.

The LDA yields a simple A dependence based on the assumption that the EMC effect scales with density. Since this is not expected to work for light nuclei, one can instead use the average nuclear density based on calculations or electron-scattering measurements of the nuclear mass (or charge) density. Figure 5 shows the size of the EMC effect as a function of the average nuclear density. For light nuclei ($A \leq 12$), the average density is evaluated using density distributions extracted within Green Function Monte Carlo (GFMC) calculations [52, 53], while for heavier nuclei it is derived from electron scattering

extractions of the charge density [54]. This is in contrast to Ref. [28], in which the average density was calculated assuming a uniform sphere with radius equal to the RMS charge radius of the relevant nucleus, although for $A \geq 12$, this yields the same qualitative behavior as is seen in Fig. 5.

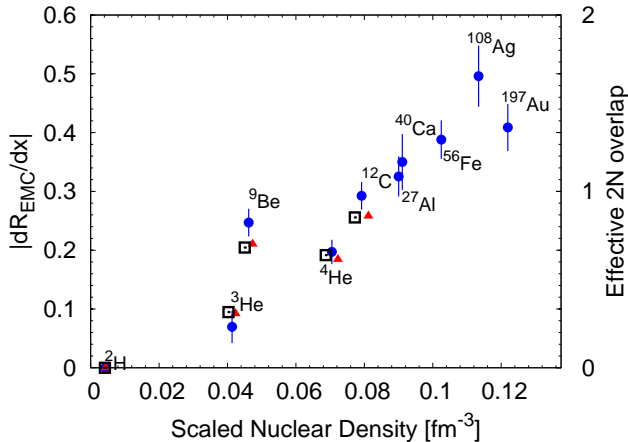


FIG. 6: (color online) Magnitude of the EMC effect vs. scaled nuclear density, which is the average nuclear density, scaled by $(A-1)/A$ to give the contribution of $A-1$ nucleons (solid circles). The solid triangles and hollow squares show the calculated average 2N overlap from Eq. 5 (See text for details). Points offset on the x -axis for clarity.

The average nuclear density yields a poor description of the data for light nuclei. In Ref. [31], a scaled nuclear density was taken, where the average density is scaled by a factor $(A-1)/A$. This was applied as a simple correction aimed at measuring the *greater* density seen by the struck nucleon due to the nuclear environment. We show the results against the scaled density in Fig. 6. The size of the EMC effect correlates very well with the scaled nuclear density, with the exception of ${}^9\text{Be}$ and the poor extrapolation to the deuteron. The former was first explained [31] as being due to the cluster-like structure of ${}^9\text{Be}$, whose wave function includes a sizable component in which the nucleus can be thought of as two α clusters associated with a single neutron [55–57]. If the EMC effect is governed by the local rather than the average nuclear density, then it is not unreasonable that the size of the effect in ${}^9\text{Be}$ would be similar in magnitude to that in ${}^4\text{He}$.

As mentioned earlier, nucleons can have a significant amount of overlap in the nucleus before they come close enough to feel the repulsive core. If we can quantify this overlap, it could be a reasonable measure of the local density. One way to estimate this effect is by taking the 2-body density distributions from GFMC calculations [52, 53] which provide the distribution of the relative nucleon separation between pp , np , and nn configurations. If we integrate the normalized $\rho_2^{pp}(r)$ up to $r = 1.7$ fm, we find the probability that a proton is within 1.7 fm (twice

the RMS radius of a nucleon) of another proton. Thus, we define a measure of the relative pair overlap between nucleons by taking

$$O_{NN} = \int_0^\infty W(r) \rho_2^{NN}(r) d^3r \quad (4)$$

as the overlap for the nn , np , and pp pairs, where $W(r)$ is a cutoff function used to evaluate the contribution at short distances. If $W(r)$ is a step function that cuts off at $r = R_0$, then O_{pn} represents the average probability that a given pn pair has a separation of R_0 or less. A proton, then, has an average overlap parameter $O_p = (Z-1)O_{pp} + NO_{pn}$, which for a step function with $R_0 \rightarrow \infty$ yields $(A-1)$, the total number of neighbor nucleons for the studied proton. To obtain the effective 2N overlap for a given reaction, we take a cross section weighted average of O_p and O_n :

$$\langle O_N \rangle = (Z\sigma_p O_p + N\sigma_n O_n) / (Z\sigma_p + N\sigma_n). \quad (5)$$

We show the effective 2N overlap for two calculations in Fig. 6. The solid triangles are for a step function with $R_0 = 1.7$ fm and $\sigma_n/\sigma_p = 0.5$, although the result is very insensitive to the exact value of σ_n/σ_p . Because the amount of overlap between nucleons decreases with the separation, $W(r)$ can be chosen to enhance the effect when the nucleons are extremely close together. The hollow squares are the result when we take $W(r)$ to be a gaussian centered at $r = 0$ with a width of 1 fm. In both cases, there is an overall normalization factor applied in order to compare to the A dependence of the EMC slopes. Both of these simple calculations of overlap yield a good qualitative reproduction of the behavior for light nuclei and which is not very sensitive to the choice of the cutoff function or the exact scale of the cutoff parameter.

To test more definitively the notion that the EMC effect depends on “local density”, additional data on light nuclei, especially those with significant cluster structure, are required. Such studies are planned as part of the program after the Jefferson Lab 12 GeV Upgrade [58]. For all of the light nuclei, an average overlap parameter can be obtained from the *ab initio* GFMC calculations. This provides realistic input of the distribution of nucleons in these nuclei, although the quantitative evaluation of the overlap parameter does depend on the somewhat arbitrary choice of the cutoff function in Eq. (4). One could also use measurements of short-range correlations in nuclei as an observable which is also sensitive to the relative contribution from short-distance configurations in nuclei. This is one possible interpretation of the correlation observed between SRC measurements and the EMC effect, and we will present this in detail after examining the A dependence of the short-range correlation measurements.

NUCLEAR DEPENDENCE OF SHORT RANGE CORRELATIONS

Much as DIS isolates scattering from quasi-free quarks, quasielastic scattering isolates incoherent scattering from the protons and neutrons in the nucleus. This allows a study the momentum distributions of the bound nucleons [59]. Inclusive electron scattering can be used to isolate contributions from high-momentum nucleons in SRCs by going to $x > 1$ kinematics [2, 11, 59].

In the QE regime, we can decompose the cross section into contributions from single-nucleon scattering (mean-field independent particle contributions) and scattering from 2-nucleon, 3-nucleon, etc... correlations [2] via:

$$\sigma(x, Q^2) = \sum_{j=1}^A A \frac{1}{j} a_j(A) \sigma_j(x, Q^2) \quad (6)$$

where $\sigma_j(x, Q^2) = 0$ at $x > j$ and the $a_j(A)$'s are proportional to the probabilities of finding a nucleon in a j -nucleon correlation. In the case of the electron-deuteron cross section, σ_2 will be dominated by contributions from 2N correlations for $x > 1.4$, where the nucleon momentum is well above k_F and the mean field contribution has died off. In this case, a_2 can be closely related to the number of 2N correlations in the nucleus (per nucleon) relative to that of the deuteron. Hence Eq. (6) expresses the fact that in the region $j < x < j + 1$ the contribution of j -nucleon SRC dominates. This result is in reasonable agreement with numerical calculations of the nuclear spectral functions [60, 61].

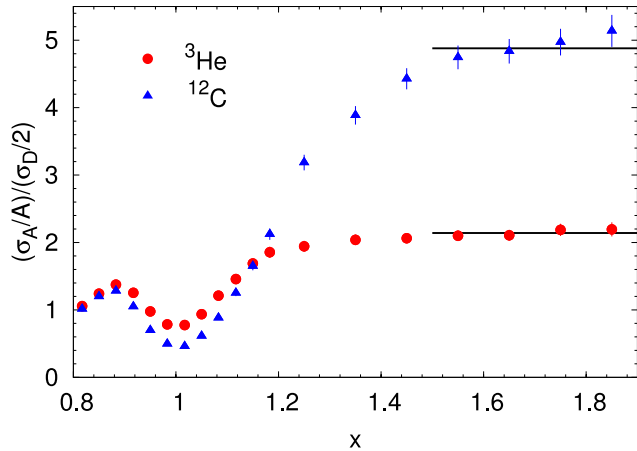


FIG. 7: (color online) Per nucleon cross section ratios for ${}^3\text{He}$ and ${}^{12}\text{C}$ measured at JLab [7] with a 5.766 GeV electron beam at a scattering angle of 18° . In the region dominated by 2N SRCs (denoted by a straight line fit, corresponding to the high momentum tail) the ratios becomes independent of x . The ratio grows with mass number A . The dip around $x=1$ is the result of $A > 2$ nuclei having wider quasielastic peaks, due to higher fermi momenta.

Equation (6) suggests scaling relations between scattering off the lightest nuclei ($A = 2$, for example) and

heavier nuclei:

$$\frac{\sigma_A(x, Q^2)/A}{\sigma_D(x, Q^2)/2} = a_2(A) \Big|_{1.4 \lesssim x \lesssim 2} \quad (7)$$

The scaling of the cross section ratios has been established, first at SLAC [2] and at Jefferson Lab [3, 4, 7]. The most recent experiment at Jefferson Lab measured this scaling precisely in the 2N correlation region for a range of nuclei with selected data shown in Figure 7.

In extracting the relative contributions of 2N-SRCs in the inclusive cross section ratios at $x > 1$, it has typically been assumed that the electron is scattering from a pair of nucleons with large relative momentum but zero total momentum, such that the cross section for scattering from a neutron-proton pair in a nucleus is identical to the cross section for scattering from a deuteron. In this case, the elementary electron-nucleon cross sections as well as any off-shell effects cancel out in taking the ratio. Final state interactions are also assumed to cancel out in the cross section ratios [2, 11].

Earlier analyses [2–4] assumed that the SRCs would be isospin-independent, with equal probability for pp , np , and nn pairs to have hard interactions and generate high-momentum nucleons. This necessitated an "isoscalar correction" to account for the excess of nn (or pp) pairs in non-isoscalar nuclei as well as the difference between the $e-p$ and $e-n$ elastic cross sections. More recently, measurements of two-nucleon knockout showed that these correlations are dominated by np pairs [6, 62] due to the fact that the bulk of the high-momentum nucleons are generated via the tensor part of the N-N interaction rather than the short-range repulsive core [63, 64]. The most recent experiment [7] to precisely measure SRCs on a range of nuclei did not apply this isoscalar correction, and presents results for previous measurements with this correction removed.

TABLE II: Existing measurements of SRC ratios, R_{2N} all corrected for c.m. motion of the pair. The second-to-last column combines all the measurements, and the last column shows the ratio a_2 , obtained without applying the c.m. motion correction. No isoscalar corrections are applied. SLAC and CLAS results do not have Coulomb corrections applied, estimated to be up to $\sim 5\%$ for the CLAS data on Fe and up to $\sim 10\%$ for the SLAC data on Au.

	E02-019	SLAC	CLAS	R_{2N} -ALL	a_2 -ALL
${}^3\text{He}$	1.93 ± 0.10	1.8 ± 0.3	–	1.92 ± 0.09	2.13 ± 0.04
${}^4\text{He}$	3.02 ± 0.17	2.8 ± 0.4	2.80 ± 0.28	2.94 ± 0.14	3.57 ± 0.09
Be	3.37 ± 0.17	–	–	3.37 ± 0.17	3.91 ± 0.12
C	4.00 ± 0.24	4.2 ± 0.5	3.50 ± 0.35	3.89 ± 0.18	4.65 ± 0.14
Al	–	4.4 ± 0.6	–	4.40 ± 0.60	5.30 ± 0.60
Fe	–	4.3 ± 0.8	3.90 ± 0.37	3.97 ± 0.34	4.75 ± 0.29
Cu	4.33 ± 0.28	–	–	4.33 ± 0.28	5.21 ± 0.20
Au	4.26 ± 0.29	4.0 ± 0.6	–	4.21 ± 0.26	5.13 ± 0.21

The per nucleon cross section ratio at large x provides a direct measure of the contribution of high-momentum nucleons relative to the deuteron. However, this is not equal to the relative number of SRCs, since in $A > 2$ nuclei, the correlated pair experiences motion in the mean field created by the rest of the nucleons. If the pair has a non-zero center-of-mass momentum, the momentum distribution of the pair will be smeared out which will flatten the top of the QE peak, lowering the low-momentum part of the distribution, but enhancing the high-momentum tail of the distribution. For example, a nucleon in iron is ≈ 4 times more likely to be part of an SRC than a nucleon in a deuteron (see Tab. II). However, the raw cross section ratio tells us that there are 4.75 times as many high momentum nucleons in iron as there are in the deuteron. This 20% enhancement [61] is the result of the c.m. motion of the correlated pair smearing out the high momentum tail in iron. The effect is illustrated in Fig. 8.

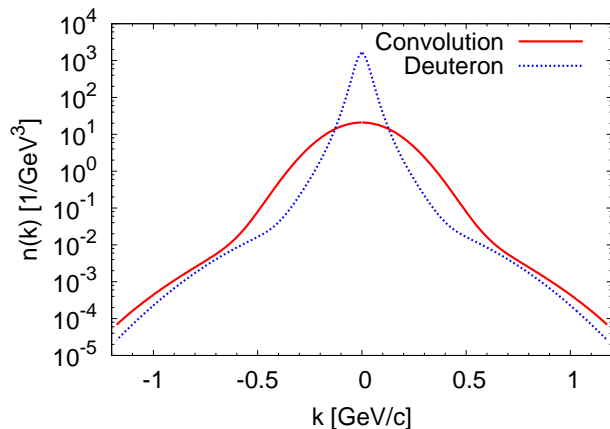


FIG. 8: (color online) Momentum distribution for the deuteron as well as the momentum distribution of the deuteron convoluted with the c.m. motion of the pair in iron [61].

A correction for this effect was first applied in Ref. [7], where analyses of previous experiments were also updated. Table II shows R_{2N} , the relative probability for a nucleon to be part of an SRC in a nucleus compared to the deuteron for each experiment (results taken from Ref. [7]), as well as an average value. We also show a_2 , the result without the correction for the c.m. motion. The meanings of the two quantities are subtly different. The raw ratio, a_2 , represents the relative strength of the high-momentum tail, i.e. the total contribution from high momentum nucleons relative to deuterium. On the other hand, c.m. motion corrected R_{2N} represents the relative number of SRCs (per nucleon) in the nucleus, relative to the deuteron. The distinction will be important in comparison of the EMC effect and SRCs in the next section.

For the purposes of this discussion, we combine the results of the JLab [7], CLAS [4] and SLAC [2] measure-

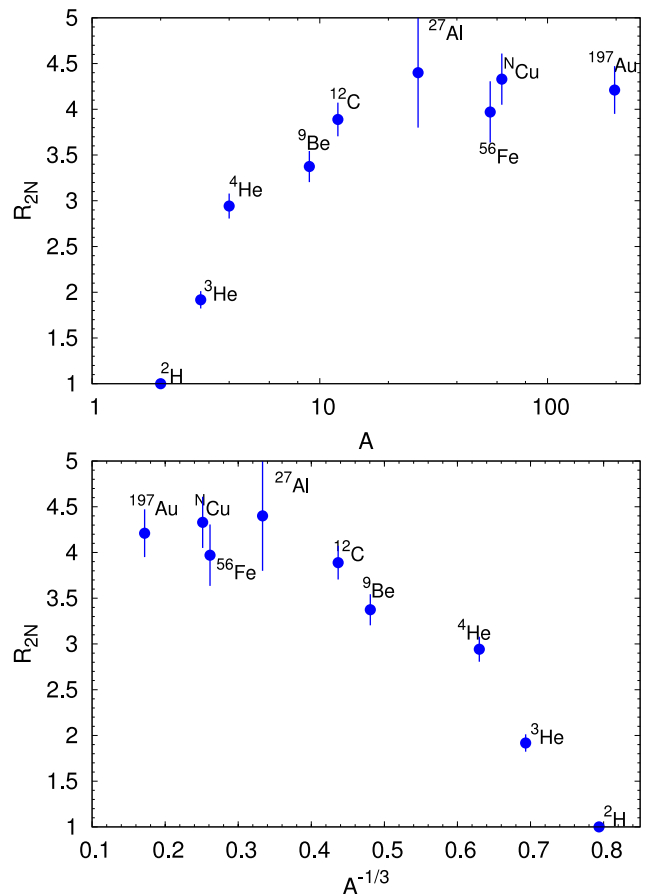


FIG. 9: (color online) R_{2N} versus A (top) and against $A^{-1/3}$ (bottom).

ments. The combined data set provides a large collection of nuclei to examine the A dependence of the extracted SRC contributions. We use R_{2N} as the measure of SRC contributions, as we are examining the behavior of the number of SRC pairs relative to the deuteron.

Figure 9 shows the A dependence of R_{2N} . The top panel shows R_{2N} vs. A , while the bottom panel shows R_{2N} as a function of $A^{-1/3}$, the behavior expected in the LDA [50, 51]. While R_{2N} is a relatively smooth function of either A or $A^{-1/3}$, there is not a simple, linear relation suggesting a proportionality to either $\ln(A)$ or $A^{-1/3}$. As with the EMC effect, the prediction of scaling with $A^{-1/3}$ is only an approximation which is not expected to be valid for very light nuclei.

For nuclei with similar form for $\rho(r)$, we expect to see scaling of the SRCs, that is, denser nuclei are more likely to have short range configurations. Figure 10 shows R_{2N} as a function of average nuclear density, discussed in the previous section. It is clear that the simple density-dependent model does not track the behavior of the light nuclei, whose large deviations that are reminiscent those shown by the EMC effect [31].

Figure 10 also shows calculation of the effective 2N

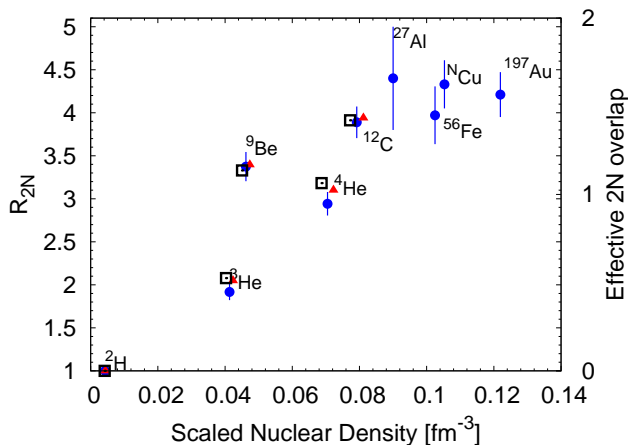


FIG. 10: (color online) R_{2N} versus average nuclear density (solid circles). The solid triangles and hollow squares show the calculated 2N overlap from Eq. 5. Points offset on the x -axis for clarity.

overlap from Eq. 5. Because the SRC measurements are designed to estimate the contribution from nucleons in short-range configurations, one would expect that them to be sensitive to the average overlap of nucleons. As can be seen, the calculated estimates of the effective 2N overlap are in very good agreement with the measured SRC contributions. This suggests that the SRC data may represent a good measure of the average overlap, allowing us to extend the comparison of the EMC effect to the average overlap to heavy nuclei, where we do not have calculations of the two-nucleon correlation functions.

DETAILED COMPARISON OF SRC AND EMC RESULTS

As discussed in the introduction, there have been previous comparisons of the nuclear dependence of the EMC and the contributions from SRCs in nuclei [25]. Given the data available at the time, the correlation seen between the two effects could be explained by a common density-dependent scaling. However, the new data on the EMC effect [31] and SRCs [7], directly compared in Fig. 11, rule out this simple explanation. For the EMC effect, it was suggested that if that the local environment of the struck nucleon drives the modification of the quark distributions, then the strong contribution of α -like clusters would make ${}^9\text{Be}$ behave like a much denser nucleus. The nearly identical behavior of ${}^9\text{Be}$ in the SRC extraction [7] supports this idea, as the SRC measurements directly probe the short-distance structure. However, even with these new data and their unexpected trend, the relationship shown in [25] still appears to be valid. This begs a careful re-examination of this linear correlation in an attempt to better understand its underlying cause.

First, we note that the initial comparison of the EMC

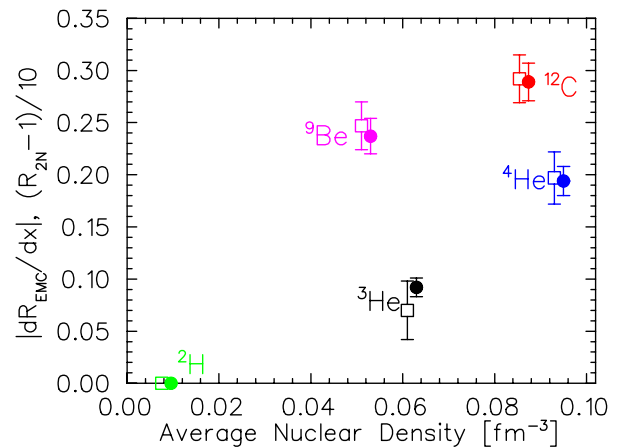


FIG. 11: (color online) Size of the EMC effect ($|dR_{EMC}/dx|$) as well as the relative measure of SRCs ($R_{2N}-1$) are shown as a function of average nuclear density. R_{2N} was scaled by an arbitrary factor.

effect and SRCs used extractions of the SRCs which included an isoscalar correction for nuclei with unequal numbers of protons and neutrons and did not apply corrections for CM motion of the correlated pair. It has been shown that SRCs are made-up of predominantly np pairs due to the tensor interaction [6, 63, 64], making the isoscalar correction unnecessary. The question of the CM motion correction is somewhat more complicated in the context of the direct comparison of the EMC and SRC results. Whether or not this correction should be applied in this analysis depends on exactly what correlation is being examined, and so we focus now on the different explanations for this correlation.

The fact that ${}^9\text{Be}$ so obviously violates the density dependence for both effects in the same way suggests that an altered density dependence, such as “local density” (LD) may give us a good description of both effects. One should then compare the size of the EMC effect to R_{2N} , which represents the relative probability that a nucleon will be part of a very short-distance configuration (a deuteron-like SRC). While high-momentum nucleons are primarily generated by np pairs, all short-distance NN pairs contribute to high local density. In the “local density” picture, we would expect that the EMC effect should scale with the number of possible NN pairs in the nucleus, $N_{tot} = A(A-1)/2$, while the SRC contribution is sensitive to only the possible np pairs, $N_{iso} = NZ$. Thus, we scale the SRC ratio by a factor N_{tot}/N_{iso} to account for the difference in the pair counting for the EMC and SRC data.

A different hypothesis to explain the linear relationship between the two effects was proposed by Weinstein et al [25], suggesting that the EMC effect is driven by the virtuality of the high-momentum nucleon [10, 30]. In this case, it is the relative probability for a nucleon to have high momentum ($> k_F$) that should drive the EMC

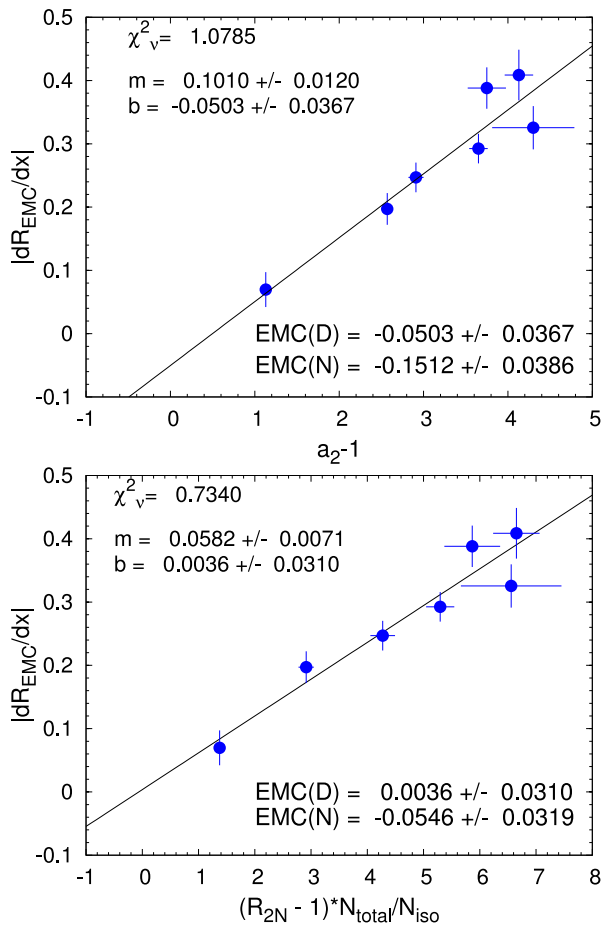


FIG. 12: (color online) Comparison of EMC slopes and SRC observables from world’s data where both observables are available for the same nuclei. The top plot shows the EMC slope vs. $a_2 - 1$, testing the high virtuality interpretation. The bottom plot shows the EMC slope vs. $R_{2N} - 1$, testing the local density interpretation (as discussed in the text). $EMC(D)$ and $EMC(N)$ are the fit values for the EMC effect corresponding to the deuteron and free nucleon.

effect, and thus the uncorrected a_2 SRC ratio is a more direct indicator of the underlying explanation.

We now make two comparisons to examine the relationship between the EMC effect and SRCs using these two different underlying assumptions. To test the high virtuality (HV) hypothesis, we use a_2 , the uncorrected ratio of A/D cross sections. We compare a_2 directly to the size of the EMC effect, as both are expected to be driven by the abundance of high momentum nucleons relative to the deuteron. To test the LD hypothesis, we correct a_2 for the CM motion of the correlated pair to get R_{2N} - the number of at-rest $2N$ SRC pairs in a nucleus relative to the deuteron. We scale it by a factor of N_{tot}/N_{iso} to reflect the fact that there more total nucleon pairs that contribute to the EMC effect than there are np pairs that form SRCs.

The data as well as the linear fits for both approaches are shown in Fig. 12. A two-parameter linear fit is per-

formed for the two approaches without any constraint for the deuteron. Thus, we can examine the fit to test both the linear correlation of the observables and the extrapolation to the expected deuteron value. The intercept of the fit is expected to be zero, since both the EMC effect and SRC contributions are taken relative to the deuteron.

Both approaches yield reasonable results, but we have to delve into the details to understand the impact of the small differences. While the LD fit has a better χ^2_{ν} value, the fractional errors of the points of the x -axis are larger due to the additional model-dependent uncertainties arising from the c.m. motion correction [7]. The uncertainties applied for this A -dependent correction are somewhat conservative and any error made in this correction is likely to have a smooth A dependence, so treating these as uncorrelated errors will artificially lower the χ^2_{ν} value. If we repeat the LD fit in Fig. 12 neglecting this extra model-dependent uncertainty (i.e. taking the same fractional uncertainty on R_{2N} as we use for a_2), the reduced χ^2_{ν} value increases to 0.88, as compared to 1.08 for the HV fit. Overall, the LD fit appears to do a better job: the extrapolation of the fit to the deuteron gives essentially zero, as it should, and it has a smaller χ^2 value. However, neither of these differences is enough to rule out the HV hypothesis.

Next, we remove the intercept as a free parameter (leaving only the slope), and thus constrain the fit by forcing it to go through zero. The χ^2_{ν} of this fit should test both the linearity and the consistency with the deuteron, allowing for a more quantitative comparison of the results. This approach more closely reflects the analysis of [25], where a one-parameter fit along with a deuteron constraint is employed. Their analysis is comparable to our HV analysis, in that they used a_2 as the measure of SRCs and the raw EMC effect slope. However, they used the older extractions of a_2 [4] which applied the isoscalar correction that we now know is not appropriate. Additionally, these extractions also involved a largely theoretical correction to go from $A/{}^3\text{He}$ ratios to $A/{}^2\text{H}$ ratios, which may be inconsistent with their inclusion of the isoscalar correction [11].

Our results for the constrained fit can be seen in Fig. 13. The gap in the χ^2_{ν} values for the two approaches grows, with 1.3 for HV and 0.61 (0.73 when taking fractional uncertainties from HV case) for LD fits. While the LD interpretation yields a better description of the data, $\chi^2_{\nu} = 1.30$ for the HV fit corresponds to a 25% confidence level, so the data are consistent with either hypothesis.

While this is a useful way to compare the relative quality of fits for the LD and HV inspired foundations, it yields an unrealistic estimate for the uncertainties on the fit. Including a deuteron constraint point neglects the fact that there are significant correlated uncertainties in all of the EMC or SRC points from a single experiment, since all of the values are measured relative to the deuteron. Therefore, the statistical and systematic

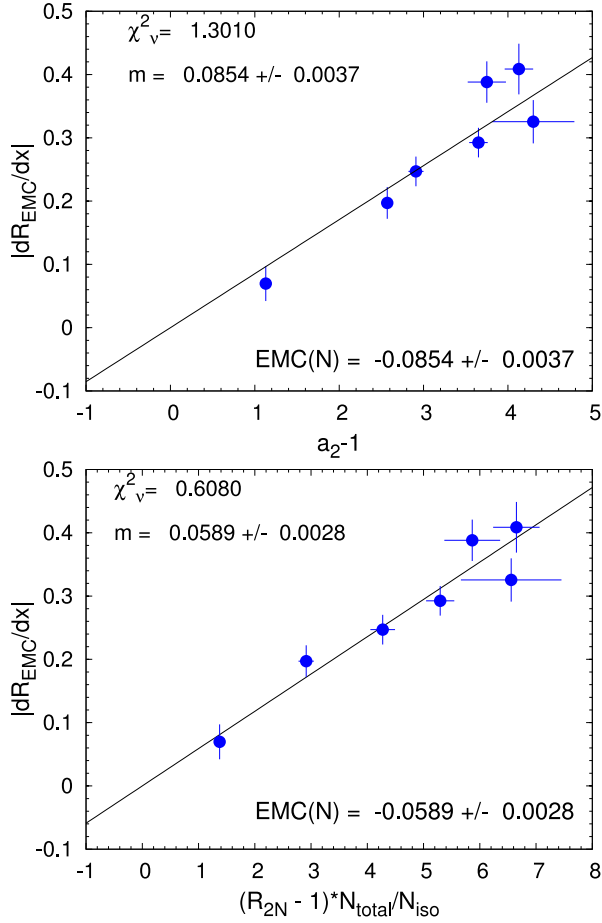


FIG. 13: (color online) EMC slopes vs a_2-1 (top) and $R_{2N}-1$ (bottom). The fit is constrained to yield zero for the deuteron.

uncertainties in the deuteron data generate an overall normalization of the values for all other nuclei from that measurement which is neglected entirely in this approach. In addition, by putting in a deuteron constraint point with no uncertainty, the linear fit will have extremely small uncertainties for all nuclei close to the deuteron, and would thus yield an uncertainty on the EMC slope that is significantly smaller than any existing measurement for light nuclei.

We can evaluate the impact of this and make a more realistic estimate of the fit uncertainties by adding a deuteron constraint point which includes a reasonable estimate of the uncertainty associated with the deuteron measurements in the experiments. We take $|dR_{EMC}/dx| = 0 \pm 0.01$, and $a_2 = R_{2N} = 1 \pm 0.015$, where the error bars were estimated based on deuterium cross section uncertainties from Refs. [31] and [7]. The fits are shown in Fig. 14, and the uncertainties in the slope are roughly a factor of three larger than in the fit that forces $EMC(D)=0$.

The relevant results from the fits are summarized in Table III. As mentioned in the discussion of the EMC effect data, the analyses done for JLab E03013 and SLAC

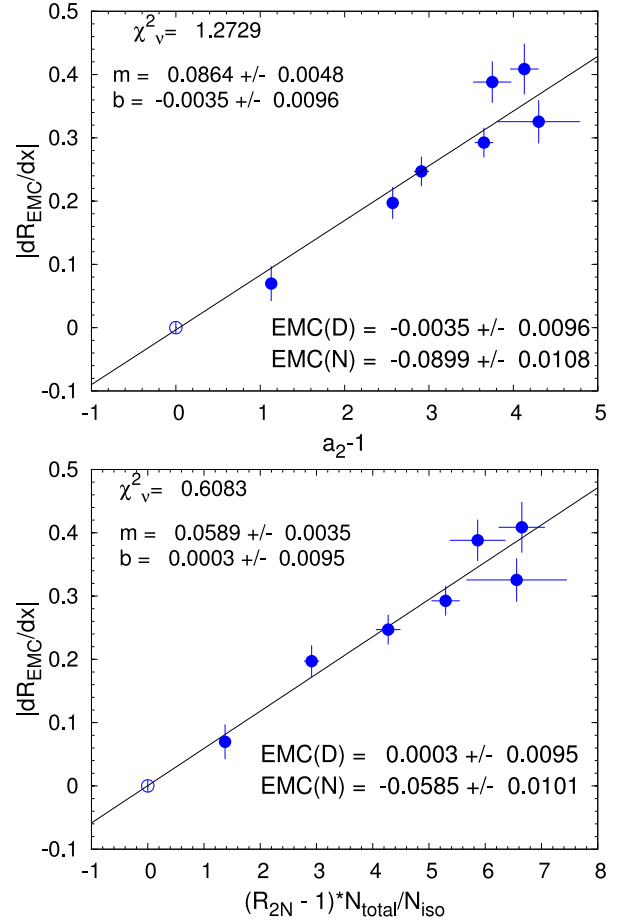


FIG. 14: (color online) EMC slopes vs a_2-1 (top) and $R_{2N}-1$ (bottom). The fit includes a constraint point with finite uncertainties for the deuteron ($|dR_{EMC}/dx|=0 \pm 0.01$; $a_2=R_{2N}=1 \pm 0.015$).

E139 used different isoscalar and Coulomb distortion corrections. We have repeated the above comparisons of the EMC and SRC measurements after estimating the impact of these differences and while the numerical results change slightly (by $\approx 10\%$ of the uncertainty), they do not affect the trends or the conclusions.

POTENTIAL IMPACT OF THE CONNECTION

The close connection between the measurements of the EMC effect and the relative contribution from short-range configurations in nuclei suggests that the modification of the nuclear quark distributions may be related to these short-range structures. However, as seen in the previous section, the connection can be made by both the HV and LD descriptions. Future measurements should allow us to better differentiate between these, but at the moment, we cannot make a definitive conclusion as to the exact nature of this connection.

In addition to helping to elucidate the origin of the

TABLE III: Summary of linear fits of EMC effect vs R_{2N} or a_2 , and extrapolations to the slopes of the EMC effect for the deuteron, EMC(D), and IMC effect for the deuteron, IMC(D). “-0” denotes a 1-parameter fit, forcing the line to go through zero, corresponding to no EMC effect for the deuteron. “-D” denotes a two parameter fit including a realistic deuteron constraint described in the text. Number in parentheses of the χ^2_ν column includes the result of fitting with smaller fractional errors from a_2 .

As Published	χ^2_ν	EMC(D)	IMC(D)
HV (Fig. 12)	1.08	-0.0503±0.037	0.1010±0.037
HV - 0 (Fig. 13)	1.30	–	0.0854±0.004
HV - D (Fig. 14)	1.27	-0.0035±0.010	0.0864±0.010
LD (Fig. 12)	0.73 (0.88)	0.0036±0.031	0.0582±0.031
LD - 0 (Fig. 13)	0.61 (0.73)	–	0.0589±0.003
LD - D (Fig. 14)	0.61 (0.73)	0.0003±0.010	0.0589±0.010

EMC effect, a better understanding of this connection will also impact other attempts to understand nuclear effects based on this relation. In particular, a better understanding of nuclear effects in the deuteron is critical to have a more reliable extraction of the free neutron structure function. In addition, details of the structure functions in light nuclei are important for measurements which use light nuclei in place of nucleon targets, e.g. the use of polarized ^3He as a substitute for a polarized neutron target.

A key aspect of the initial analysis comparing the EMC effect and SRCs [25] was the extrapolation of the EMC effect to the free nucleon, which allows the extraction of the nuclear effects in the deuteron. The authors of ref. [25] use the fit to extract the IMC (in-medium correction) effect, defined as $\frac{\sigma_A/A}{(\sigma_p+\sigma_n)/2}$, by taking the EMC slope based on the ratio to the deuteron and adding the slope associated with the IMC for the deuteron, $\sigma_d/(\sigma_p + \sigma_n)$, given by the extrapolation of the EMC/SRC linear correlation. Given the IMC for the deuteron, they extract the sum of free proton and neutron structure functions and, subsequently, $F_{2n}(x)$. They obtain an IMC slope for the deuteron of 0.079 ± 0.006 where, as discussed above, the small error is a consequence of using the known values for the deuteron as a constraint while neglecting the correlated uncertainties in the measurements. The equivalent global analysis from their later work, including the new data from Ref. [7], yields 0.084 ± 0.004 [32]. In both cases, they use a fit of the EMC slope to a_2 which is not quite consistent with either our LD or HV comparisons.

We repeat this extraction to obtain the IMC slope for the deuteron, using our fits from Figs. 12-14 and taking the difference of the EMC slope extrapolated to the free nucleon ($a_2=R_{2N}=0$) and that for the deuteron. Note that this is equivalent to the slope parameter, b , of the fits, and taking $dR_{IMC}(D) = b$ accounts for the corre-

lated errors in the EMC slopes for the deuteron and free nucleon. Similarly, one can obtain the IMC slope for $A > 2$ via $dR_{IMC}(A) = dR_{EMC}(A) + dR_{IMC}(D)$.

For both the LD and HV fits, we focus on the uncertainties from fits where the deuteron constraint is applied, but where uncertainties associated with the constraint are taken into account (Fig. 14). These are larger than the quoted uncertainties of the previous global fits which do not account for the correlated uncertainties in the EMC and SRC ratios for different nuclei. The HV approach yields slopes that are close to the earlier analyses, for fits where a constraint for the deuteron is applied. The LD fits all yield a smaller IMC slope for the deuteron, suggesting smaller nuclear effects. A reanalysis [32] of the deuteron IMC effect with different data sets found its value varied from 0.079 to 0.106, with the largest difference associated with the use of R_{2N} rather than a_2 from the SRC measurements. In the same work, the value for the IMC effect is always larger than our results based on local density because they assume that only the high-momentum nucleons associated with the SRCs contribute to the EMC effect, while low-momentum short-distance pairs are included in our local density analysis through the factor N_{tot}/N_{iso} .

The use of the SRC observables to extrapolate measurements of the EMC effect to the free nucleon generates a large range of potential results, with IMC slopes for the deuteron from 0.059 to 0.101, even under the assumption that the correlation is perfectly linear all the way to $A = 2$. However, this range is significantly narrowed if one can determine whether the underlying connection is related to the density or the virtuality associated with the short-distance configurations. With further studies, this may be possible. If so, the nuclear effects as extrapolated from measurements can be compared with direct calculations of the nuclear effects in the deuteron. A recent study of the model dependence of nuclear effects in the deuteron [65], based on convolution calculations and off-shell effects, produced a range of results for the neutron structure function. For on-shell extractions it is relatively narrow, and a direct comparison to the IMC for the deuteron based on extrapolation from heavier nuclei can provide a constraint on off-shell effects.

However, one must be careful in using this approach to obtain the free neutron structure function, especially at large x values. As discussed in Ref. [65], extrapolations of the EMC effect to the deuteron neglect Fermi motion, which is the dominant effect at $x > 0.6$ and is sensitive to the difference between proton and neutron structure functions at smaller x values. The Fermi motion effects have a significant Q^2 dependence in this high- x region [66, 67], limiting the reliability of such extrapolations. This may explain the change in the x dependence of the quark $d(x)/u(x)$ ratio between the IMC-based extraction [68] and the results of all the deuteron calculations examined in that work. Thus, it is necessary to

improve our understanding of the connection between the EMC effect and the presence of SRCs, to better constrain the extrapolation, and to explicitly account for the both effects of Fermi motion and additional nuclear effects, as done in Ref. [40], when going to large x values.

Additionally, Fermi motion could also impact those extractions of neutron structure functions that rely on a comparison of deep-inelastic scattering from ${}^3\text{He}$ and ${}^3\text{H}$ [69, 70]. It was shown in Ref. [69] that the difference between the nuclear effects in ${}^3\text{He}$ and ${}^3\text{H}$, defined as $\sigma_A/(Z \times \sigma_p + N \times \sigma_n)$, is extremely small, with the super-ratio of the ${}^3\text{He}$ and ${}^3\text{H}$ nuclear effects typically less than 1% from unity, with a spread of 1% when varying (variety of factors). In fact, almost all of this effect comes from the different x dependences of F_{2n} and F_{2p} , so even the simple convolution calculation of Fermi smearing yields a larger enhancement for the neutron, which falls off more rapidly with x .

Both the local-density and the high-virtuality explanations for the correlation suggest the possibility that the EMC effect will be different for protons and neutrons in non-isoscalar nuclei such as ${}^3\text{H}$ or ${}^3\text{He}$. Given the strong dominance of np pairs [6] as the source of high-momentum nucleons, the high-momentum tail of the ${}^3\text{He}$ momentum distribution would come from the single neutron interacting with one of the two protons. This implies that the neutron will be at very high momentum twice as often as either of the protons, and thus have a much higher average virtuality. Ref. [69] does account for the difference in the calculated proton and neutron momentum distributions, and thus includes the excess of the high-momentum tail in the singly-occurring nucleon. However, any effects beyond the convolution which are related to the high-momentum nucleons (or high-density configurations) will yield an additional difference in the EMC effect for protons and neutrons in $A = 3$ nuclei.

If we assume that the EMC effect for the singly-occurring nucleon is twice that of the doubly-occurring nucleon, then we can estimate the different sizes of the EMC effect in ${}^3\text{He}$ and ${}^3\text{H}$. For $x \approx 0.7$, where the proton cross section is three times the neutron cross section, one finds that the EMC effect in ${}^3\text{H}$ is 40% larger than ${}^3\text{He}$. This would likely enhance the difference between ${}^3\text{He}$ and ${}^3\text{H}$, relative to the calculations of Ref. [69], although whatever part of the EMC effect is explained by just the convolution is accounted for in their result.

Realistic calculations of the nucleon momentum distributions in ${}^3\text{He}$ (Fig 2 in Ref. [11]) show that for 300-600 MeV/c, the range which accounts for the bulk of the SRC contributions, the momentum distribution of a proton in ${}^3\text{He}$ is roughly 1.6–1.8 times the momentum distribution of a neutron. So, the effect is likely to be smaller than the estimate from the simple assumption of total np dominance. The local density picture also gives a difference if the singly-occurring nucleon has a different probability to be in a small-sized configuration than a double-

occurring nucleon. Based on GFMC calculations [52] of the two-body densities in ${}^3\text{He}$, the np pair has approximately 50% more contribution for nucleon separations below 1 fm than the pp pair, again yielding an excess of protons in high-density configurations.

SUMMARY AND CONCLUSIONS

We examined the A dependence of both the EMC effect and presence of short-range correlations in nuclei and find that the traditional models of a simple density or A dependence fail with the inclusion of the new data on light nuclei. Both observables show similar behavior, suggesting a common origin. We examine the correlation between the two observables under two different assumptions for the underlying physics. In the first, we assume that the EMC effect is driven by the presence of high-momentum nucleons in the nucleus, which is directly extracted in the inclusive measurements at $x > 1$. In the second, we assume that the EMC effect scales with the average local density, and thus correlates with the number of SRCs extracted from the $x > 1$ measurements. We find that under both assumptions, the data are consistent with a linear correlation between the two effects, with the local density comparison yielding a smaller χ^2_ν value.

These results support the local density explanation proposed in Ref. [31], but are still consistent with the explanation in terms of high virtuality [25]. In the end, a more definitive determination of the underlying physics will require further data. A large step in this direction will be taken at JLab after the 12 GeV upgrade. A large repertoire of nuclear targets, including several light nuclei with significant cluster structure, will be used to make high precision measurements of the EMC effect [58] as well as SRCs [71], which will further illuminate the nature of the relationship between the two. In addition, measurements probing the modification of nucleon form factors [18, 72] and structure functions [73, 74] as a function of virtuality are planned that will cover a large range of initial momentum, allowing for direct comparison to models of the nuclear effects.

ACKNOWLEDGEMENTS

We would like to thank Wally Melnitchouk, Doug Higginbotham, Larry Weinstein, Don Geesaman, Or Hen, and Eli Piassetzky for fruitful discussions. Also, we would like to thank Sergey Kulagin for providing calculations of separation energies used in our analysis.

This work supported by the U.S. DOE through contracts DE-AC02-06CH11357, DE-AC05-06OR23177, and DE-FG02-96ER40950 and research grant PHY-0653454 from the National Science Foundation.

-
- [1] W. Czyrs and K. Gottfried, *Ann. Phys.* **21**, 47 (1963).
- [2] L. L. Frankfurt, M. I. Strikman, D. B. Day, and M. Sargsian, *Phys. Rev. C* **48**, 2451 (1993).
- [3] K. S. Egiyan et al., *Phys. Rev. C* **68**, 014313 (2003).
- [4] K. S. Egiyan et al., *Phys. Rev. Lett.* **96**, 082501 (2006).
- [5] R. Shneor et al., *Phys. Rev. Lett.* **99**, 072501 (2007).
- [6] R. Subedi et al., *Science* **320**, 1476 (2008), 0908.1514.
- [7] N. Fomin et al., *Phys. Rev. Lett.* **108**, 092502 (2012).
- [8] J. Arrington et al., *Phys. Rev. Lett.* **82**, 2056 (1999).
- [9] J. Arrington et al., *Phys. Rev. C* **64**, 014602 (2001).
- [10] M. M. Sargsian et al., *J. Phys.* **G29**, R1 (2003).
- [11] J. Arrington, D. Higinbotham, G. Rosner, and M. Sargsian (2011), arXiv:1104.1196.
- [12] R. Machleidt, *Phys. Rev. C* **63**, 024001 (2001).
- [13] M. Lacombe, B. Loiseau, J. M. Richard, R. V. Mau, J. Côté, P. Pirès, and R. de Tournel, *Phys. Rev. C* **21**, 861 (1980).
- [14] R. B. Wiringa, V. G. J. Stoks, and R. Schiavilla, *Phys. Rev. C* **51**, 38 (1995).
- [15] X. Zhan et al., *Phys. Lett.* **B705**, 59 (2011).
- [16] G. Van Der Steenhoven et al., *Phys. Rev. Lett.* **57**, 182 (1986).
- [17] S. Strauch et al., *Phys. Rev. Lett.* **91**, 052301 (2003).
- [18] M. Paolone, S. Malace, S. Strauch, I. Albayrak, J. Arrington, et al., *Phys. Rev. Lett.* **105**, 072001 (2010).
- [19] R. D. Mckeown, *Phys. Rev. Lett.* **56**, 1452 (1986).
- [20] I. Sick, *Nucl. Phys.* **A434**, 677C (1985).
- [21] J. Jourdan, *Nucl. Phys.* **A603**, 117 (1996).
- [22] J. Morgenstern and Z. Meiziani, *Phys. Lett.* **B515**, 269 (2001).
- [23] J. Carlson, J. Jourdan, R. Schiavilla, and I. Sick, *Phys. Rev. C* **65**, 024002 (2002).
- [24] J. Aubert et al., *Phys. Lett.* **B123**, 275 (1983).
- [25] L. Weinstein, E. Piasetzky, D. Higinbotham, J. Gomez, O. Hen, and R. Shneor, *Phys. Rev. Lett.* **106**, 052301 (2011).
- [26] D. F. Geesaman, K. Saito, and A. W. Thomas, *Ann. Rev. Nucl. Sci.* **45**, 337 (1995).
- [27] P. R. Norton, *Rept. Prog. Phys.* **66**, 1253 (2003).
- [28] J. Gomez et al., *Phys. Rev. D* **49**, 4348 (1994).
- [29] F. Gross and S. Liuti, *Phys. Rev. C* **45**, 1374 (1992).
- [30] C. Ciofi degli Atti, L. Frankfurt, L. Kaptari, and M. Strikman, *Phys. Rev. C* **76**, 055206 (2007).
- [31] J. Seely et al., *Phys. Rev. Lett.* **103**, 202301 (2009).
- [32] O. Hen, E. Piasetzky, and L. Weinstein (2012), arXiv:1202.3452.
- [33] G. Piller and W. Weise, *Phys. Rept.* **330**, 1 (2000).
- [34] A. Aste, C. von Arx, and D. Trautmann, *Eur. Phys. J.* **A26**, 167 (2005).
- [35] P. Solvignon, D. Gaskell, and J. Arrington, *AIP Conf. Proc.* **1160**, 155 (2009), arXiv:0906.0512.
- [36] S. Dasu et al., *Phys. Rev. D* **49**, 5641 (1994).
- [37] A. Daniel et al., in preparation.
- [38] P. Solvignon et al., in preparation.
- [39] S. A. Kulagin and R. Petti, *Phys. Rev. C* **82**, 054614 (2010).
- [40] S. A. Kulagin and R. Petti, *Nucl. Phys.* **A765**, 126 (2006).
- [41] R. P. Bickerstaff and W. Thomas, A., *J. Phys.* **G15** (1989).
- [42] D. S. Koltun, *Phys. Rev. C* **9**, 484 (1974).
- [43] G. L. Li, K. F. Liu, and G. E. Brown, *Phys. Lett.* **B213**, 531 (1988).
- [44] S. Akulinichev, G. Vagradov, and S. A. Kulagin, *JETP Lett.* **42**, 127 (1985).
- [45] S. Kulagin, private communication.
- [46] J. R. Smith and G. A. Miller, *Phys. Rev. C* **65**, 055206 (2002).
- [47] J. R. Smith and G. A. Miller, *Phys. Rev. C* **66**, 049903 (2002).
- [48] O. Benhar, V. R. Pandharipande, and I. Sick, *Phys. Lett.* **B410**, 79 (1997).
- [49] O. Benhar, A. Fabrocini, and S. Fantoni, *Nucl. Phys.* **A505**, 267 (1989).
- [50] A. Antonov and I. Petkov, *Il Nuovo Cimento A* (1971-1996) **94**, 68 (1986).
- [51] I. Sick and D. Day, *Phys. Lett.* **B274**, 16 (1992).
- [52] S. C. Pieper and R. B. Wiringa, *Ann. Rev. Nucl. Part. Sci.* **51**, 53 (2001).
- [53] S. Pieper, private communication.
- [54] H. De Vries, C. W. De Jager, and C. De Vries, *Atom. Data Nucl. Data Tabl.* **36**, 495 (1987).
- [55] K. Arai, Y. Ogawa, Y. Suzuki, and K. Varga, *Phys. Rev. C* **54**, 132 (1996).
- [56] M. Hirai, S. Kumano, K. Saito, and T. Watanabe, *prc.* **83**, 035202 (2011).
- [57] S. Pandit, V. Jha, K. Mahata, S. Santra, C. Palshetkar, et al., *prc.* **84**, 031601 (2011).
- [58] J. Arrington, A. Daniel, and D. Gaskell, Jefferson Lab experiment E12-10-008.
- [59] O. Benhar, D. Day, and I. Sick, *Rev. Mod. Phys.* **80**, 189 (2008).
- [60] C. C. degli Atti et al., *Phys. Rev. C* **44**, R7 (1991).
- [61] C. C. degli Atti and S. Simula, *Phys. Rev. C* **53**, 1689 (1996).
- [62] E. Piasetzky, M. Sargsian, L. Frankfurt, M. Strikman, and J. Watson, *Phys. Rev. Lett.* **97**, 162504 (2006).
- [63] M. M. Sargsian, T. V. Abrahamyan, M. I. Strikman, and L. L. Frankfurt, *Phys. Rev. C* **71**, 044615 (2005).
- [64] R. Schiavilla, R. B. Wiringa, S. C. Pieper, and J. Carlson, *Phys. Rev. Lett.* **98**, 132501 (2007).
- [65] J. Arrington, J. Rubin, and W. Melnitchouk (2011), arXiv:1110.3362.
- [66] J. Arrington, F. Coester, R. Holt, and T.-S. Lee, *J. Phys.* **G36**, 025005 (2009).
- [67] A. Accardi, M. Christy, C. Keppel, P. Monaghan, W. Melnitchouk, J. Morfin, and J. Owens, *Phys. Rev. D* **81**, 034016 (2010).
- [68] O. Hen, A. Accardi, W. Melnitchouk, and E. Piasetzky, *Phys. Rev. D* **84**, 117501 (2011).
- [69] I. R. Afnan et al., *Phys. Rev. C* **68**, 035201 (2003).
- [70] G. G. Petratos, J. Gomez, R. J. Holt, and R. D. Ransom, Jefferson Lab experiment E12-10-103.
- [71] J. Arrington and D. Day, Jefferson Lab experiment E12-06-105.
- [72] E. Brash, G. M. Huber, R. Ransome, and S. Strauch, Jefferson Lab experiment E12-11-002.
- [73] A. V. Klimenko et al., *Phys. Rev. C* **73**, 035212 (2006).
- [74] O. Hen, L. B. Weinstein, S. Gilad, and S. A. Wood, Jefferson Lab experiment E12-11-107.